RSC Advances

PAPER

View Article Online
View Journal | View Issue

Cite this: *RSC Adv.*, 2024, **14**, 26457

Adsorption of oral antibacterial agents on zirconia surfaces with different crystal systems†

Mihiro Itotagawa,[ab] Hiroshi Kono,[*b] Tadahiro Higashinakao,[b] Yuki Sugiura,[c] Yuta Otsuka,[b] Masafumi Kikuchi[b] and Yoshihiro Nishitani[a]

Zirconia ceramics are widely used as dental prosthetics owing to their high biocompatibility, excellent mechanical strength, and aesthetic properties similar to color tones of natural teeth. However, there exists a growing demand for the facile attachment of antibacterial properties in long-term dental restoration. Thus, in this study, we evaluated the adsorption ability of cetylpyridinium chloride (CPC) and benzalkonium chloride (BKC)—quaternary amines widely used as antibacterial substances in commercial toothpaste and other oral care products—onto zirconia surfaces with tetragonal and monoclinic crystal structures. Although tetragonal zirconia has been widely used in dental prosthetic materials such as crowns *etc.*, monoclinic zirconia has also been used under oral conditions because of long-term implantation. When antibacterial molecule loading on zirconia powders under simulated oral conditions, it was revealed that monoclinic zirconia adsorbed approximately five times more CPC and BKC per unit area compared with that of tetragonal zirconia. Moreover, in tetragonal zirconia, the adsorption amounts of both CPC and BKC increased slightly with growing Y_2O_3 content as a stabilizer. This phenomenon was attributable to the formation of complexes between rare earth elements (REE) such as Y_2O_3 in zirconia and quaternary amines such as CPC and BKC. In this study, the antibacterial molecular adsorption ability of dental zirconia was observed, and new advantages of zirconia in dental applications were discovered.

Received 4th June 2024
Accepted 11th August 2024

DOI: 10.1039/d4ra04084h

rsc.li/rsc-advances

Introduction

Dental caries remains one of the most prevalent oral health issues. Thus, conservative restoration and prosthetic treatment for dental caries are essential in dental care. Dental restoration materials typically offer sufficient strength and aesthetic properties.[1,2] Thus, recent research on dental medicine has been focused on preventing marginal leakage of such materials as well as secondary dental caries, along with achieving an enhanced oral environment over the long term. Studies on the loading of antibacterial agents in adhesive materials have demonstrated that improved bonding between dentin and dental restoration materials can help prevent marginal leakage and secondary caries.[3–5]

However, the prolonged use of dental restorations typically leads to the depletion of antibacterial substances within these materials, causing a notable clinical problem. Despite advancements in dental materials, the survival rate of restored crowns after 10 years is less than 70% at present.[6] The need for re-treatment of crown restorations owing to secondary caries poses a significant burden, especially to elderly patients. Furthermore, depending on the depth of caries, tooth extraction may be required.[7] Given the global trend of an aging population and the long-term use of dental restorations in oral cavities, there is a growing need for developing sustainable and easy-to-use antibacterial solutions that can be adsorbed onto dental restorations for preventing caries and maintaining quality of life (QOL).

Zirconia ceramics have emerged as an attractive solution in dental applications owing to their aesthetic appeal, excellent mechanical properties, and biocompatibility. Consequently, these materials have been applied in anterior teeth and all-ceramic crowns for dental prostheses.[8–12] Pure zirconia (ZrO_2) exhibits three phases with different crystal systems depending on the temperature: monoclinic (below 1170 °C), tetragonal (1170–2370 °C), and cubic (above 2370 °C).[13] Although at room temperature, the monoclinic phase is stable, the additive of oxides (several at%), such as CeO_2, Y_2O_3, and CaO, enables the stabilization of the tetragonal phase below phase transition

[a]*Department of Restorative Dentistry and Endodontology, Graduate School of Medical and Dental Sciences, Kagoshima University, 8-35-1 Sakuragaoka, Kagoshima, Kagoshima 890-8544, Japan*

[b]*Department of Biomaterials Science, Graduate School of Medical and Dental Sciences, Kagoshima University, 8-35-1 Sakuragaoka, Kagoshima, Kagoshima 890-8544, Japan. E-mail: hiro164@dent.kagoshima-u.ac.jp*

[c]*Health and Medical Research Institute, National Institute of Advanced Industrial Science and Technology (AIST), 1-1-1 Higashi, Tsukuba, Ibaraki 305-0035, Japan*

† Electronic supplementary information (ESI) available. See DOI: https://doi.org/10.1039/d4ra04084h

temperatures (Fig. 1).[8,14,15] Since, tetragonal zirconia, which is partially stabilized by Y_2O_3, exhibits high strength and toughness, it has been widely used for dental restorations.[16] In particular, the superior properties of tetragonal zirconia are due to a unique process in which part of the energy of the impact is used for facilitating the transition to the monoclinic phase and subsequent expansion.[17–19] However, neither zirconia nor its stabilizing elements themselves possess any antibacterial properties.

Attaching antibacterial properties, commercial toothpastes, mouthwashes, and throat lozenges typically contain quaternary amines ($-NR_3^+$), such as cetylpyridinium chloride [CPC: $C_5H_5(N^+)-(CH_2)_{15}-CH_3\cdot Cl$] and benzalkonium chloride [BKC: $C_6H_5CH_2(N^+)(CH_3)_2R\cdot Cl$ ($R = C_8H_{17}-C_{18}H_{37}$)] as antibacterial agents, known for their broad-spectrum antibacterial properties.[20–22] These quaternary amines also form complexes with numerous metal ions.[23–25] Thus, the coordination of antibacterial molecules with zirconium and other ions exposed on the zirconia surface can potentially result in an antibacterial film that can be replenished through routine oral care.

Considering these aspects, this study aimed to examine the adsorption of antibacterial quaternary amine molecules on the surface of zirconia. We employed tetragonal zirconia as immediately after setting dental restorations in the oral cavity as and monoclinic zirconia as after long-term use, respectively. The relationship between the crystal systems of zirconia and the adsorption of antibacterial quaternary amine molecules was evaluated.

Materials and methods

Preparation of zirconia powders with different crystal systems

ZrO_2 powders with different contents of Y_2O_3 (TZ-PX-245, TZ-PX-524, and TZ-PX-430) were obtained from Tosoh Co. (Tokyo, Japan). All other reagents including ZrO_2 (without Y_2O_3) were purchased from FUJIFILM Wako Pure Chemical Co. (Osaka, Japan). For ease of reference, based on their Y_2O_3 contents, TZ-PX-245, TZ-PX-524, and TZ-PX-430 are denoted as 3Y-TZP, 4Y-TZP, and 6Y-TZP, respectively. The ZrO_2 powder was placed in an alumina firing dish and burned at 600 °C for 10 h. While the 3Y-TZP, 4Y-TZP, and 6Y-TZP powders were burned at 1100 °C for 5 h to induce phase conversion and remove any residual organic matter.

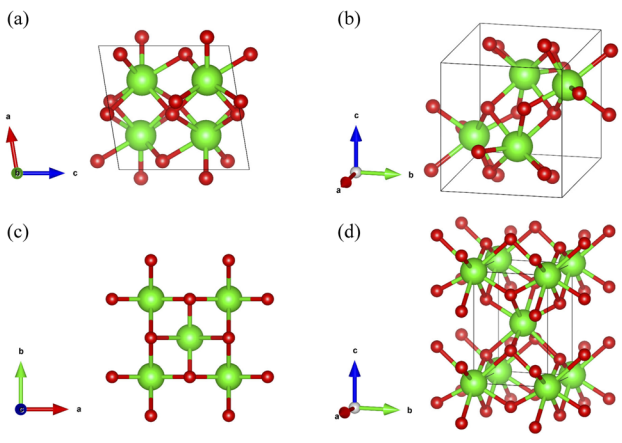

Fig. 1 Schematic illustrations of zirconia crystal structures.[14] Green and red denote zirconia and oxygen atoms, respectively. (a) Monoclinic zirconia, view toward the *b*-axis. (b) Monoclinic zirconia, view toward the *a*-axis. (c) Tetragonal zirconia, view toward the *c*-axis. (d) Tetragonal zirconia, view toward the *a*-axis.

Evaluation of complex formation

Each zirconia sample (0.33 g) was immersed in 30 mL phosphate-buffered saline (PBS) with or without 0.5 wt% CPC or BKC. The sealed samples were placed in a shaking incubator (BR-23FP, Taitek Corporation, Saitama, Japan) and agitated at 60 rpm for 24 h at 37 °C. The pH of the sample solutions was measured using a pH electrode (LAQUA-PH-SE, HORIBA Ltd., Kyoto, Japan). Subsequently, the suspensions were centrifuged at 9000 rpm in a centrifuge (AX-310, Tomy Seiko Co., Ltd., Tokyo, Japan). The supernatant fluid was then removed, washed several times with distilled water, and dried completely at 40 °C.

Characterization

The prepared samples were sputtered with Os using an Os coating apparatus for electron microscopy (HPC-1SW, Vacuum Device Inc., Ibaraki, Japan). The fine structures were observed through field-emission scanning electron microscopy (FE-SEM; JEM6700z, JEOL Ltd., Tokyo, Japan) at an acceleration voltage of 3 kV and a current of 20 μA. Crystallographic properties were assessed through analysis of the X-ray diffraction (XRD) pattern (MiniFlex 600, Rigaku Corporation, Tokyo, Japan) measured in the 2θ range of 20° to 80° using Cu–Kα radiation, an acceleration voltage of 40 kV, and a current of 15 mA, at a measurement rate of 5° min^{-1}. The chemical composition of the prepared samples was determined through X-ray fluorescence analysis (XRF) (EDX-8100, Shimadzu Corporation, Kyoto, Japan) at an acceleration voltage of 50 kV under vacuum conditions. The specific surface area of the fabricated samples, known to influence the complexation ability, was measured using the Brunauer–Emmett–Teller (BET) method (NOVA1200e, Anton Paar Inc., Florida, USA).[26] The samples were evacuated overnight at room temperature, and nitrogen was introduced in eleven pressure steps ($P/P_0 = 0.05–0.90$) at −196 °C.

To evaluate the amount of CPC and BKC adsorbed, the samples were subjected to carbon–hydrogen–nitrogen (CHN) elemental analysis (CHN coder MT-6, Yanaco Analytical Industries, Kyoto, Japan) using Ar gas as a carrier.

The thermal stability of the samples was determined by thermogravimetry–differential thermal analysis (TG-DTA: Thermo-Plus, TG8210, Rigaku Co., Japan). The samples were heated to 1000 °C at 10 °C min^{-1} using Al_2O_3 as the standard.

The surface potential of zirconia powder samples in PBS was evaluated through zeta potential measurements. The mass of 5.00 mL of each of the prepared samples was measured, and the mass of 50.0 μL of each sample was calculated from the computed density. Subsequently, 50.0 μL of each sample was ground in an alumina mortar with a small amount of PBS as a lubricant to form a slurry. Each ground sample was immersed

in 50.0 mL of PBS diluted 10-fold with distilled water to prepare a 0.1 vol% solution. Each solution was stirred using a vortex mixer (VMX-3000V, As One Corporation, Osaka, Japan) for 1 min. The zeta potential of each solution was then measured using a zeta potential measurement phase (ELSZ-2000, Otsuka Electronics Co., Ltd., Osaka, Japan). A high-power semiconductor laser was used, and the measurement was performed at a solvent temperature of 25 °C. A standard quartz cell unit (ELSZ series, Otsuka Electronics Co., Ltd) was used as the cell.

Antibacterial test

We performed an antibacterial activity test with prior approval from the AIST microbial experiment ethical committee (approval number: B2019-0110-D, B2019-0113-E). We chose *Staphylococcus aureus* (NBRC100910T) as the representative Gram-positive bacteria. This antibacterial test was modified from the standard methods of ISO 22196:2011. The bacteria were cultured in the Bouillon medium (Pearl-core Heart Infusion, Eiken Co., Tokyo, Japan) at 37 °C for 1 day.

Commercially available Ceramil HT^{+} (Amann Girrbach, Koblach, Austria) made from 4Y-TZP was used as the zirconia sample. Commercially available Ceramil zolid fx (Amann Girrbach, Koblach, Austria) made from 6Y-TZP was used as the zirconia sample. Cylindrical-shaped zirconia blocks were cut into discs by an automatic precision cutting machine (Isomet, Buehler Ltd, IL, USA). The discs were sintered at 1450 °C for 2 h (rate of increase = 8 °C min^{-1}) in accordance with the specified manufacturer's conditions. After sintering, the discs were prepared to 10 mm in diameter and 0.6 mm thickness, and the surfaces were automatically polished (Ecomet 250, Buehler Ltd, IL, USA) with #400-1200 polishing paper for 5 min. Next, the samples were mirror polished using a dental rubber polishing bar (Zircoshine, Shofu Inc., Kyoto, Japan). The samples were then autoclaved at 120 °C for 15 min and then immersed in 10 wt% BKC for 10 min. The samples that were not immersed BKC but were immersed in 70% ethanol were used as control. The samples were then washed several times with sterilized PBS.

The samples were placed on a medium coated with each bacterium and incubated at 37 °C for 24 h to evaluate the inhibition circular formation ability.

Statistical analysis

All statistical analyses were performed using IBM SPSS Statistics 27, with $\alpha = 0.05$. A two-way analysis of variance (ANOVA) was performed to assess the carbon adsorption per unit area of the samples after the immersion test. Tukey's test was conducted to examine the significant p values. One-way ANOVA was performed on the zeta potentials of the zirconia samples in PBS after the immersion test. Additionally, one-way ANOVA was performed on the results of the antibacterial test.

Results and discussion

First, the crystal structures of the zirconia ceramic powder samples used in the immersion experiments were evaluated.

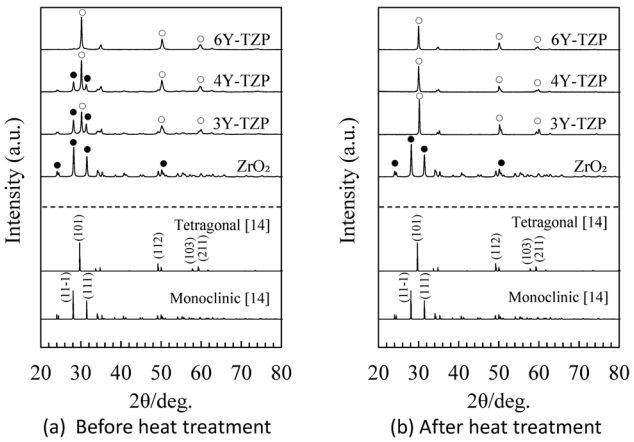

Fig. 2 XRD patterns of the zirconia samples for immersion test before (a) and after (b) heat treatment. The peaks marked as ● indicate the monoclinic phase and peaks marked as ○ indicate the tetragonal phase.

Fig. 2(a) and (b) show the XRD patterns of the zirconia ceramics before and after heat treatment, respectively. The XRD patterns of monoclinic and tetragonal zirconia are also shown as ref. 14 Before heat treatment, the ZrO2 sample exhibited peaks at 27.6° and 31.8°, corresponding to the monoclinic phase. Both 3Y-TZP and 4Y-TZP exhibited the strongest peak at 30.0° and weaker peaks at 27.6° and 31.8°, indicating a tetragonal phase with mixed monoclinic phase. In contrast, 6Y-TZP presented the strongest peak at 30.0°, with extremely weak peaks at 27.6° and 31.8° compared with those of 3Y-TZP and 4Y-TZP, indicating a predominantly tetragonal phase with mixed monoclinic phase. After heat treatment, ZrO_2 exhibited peaks corresponding only to the monoclinic phase at approximately 27.6° and 31.8°, as in the case before heat treatment. In contrast, 3Y-TZP, 4Y-TZP, and 6Y-TZP presented a strong peak at 30.0° and weaker peaks at 35.0° and 50.0°. No peak corresponding to the monoclinic phase was observed, indicating a single phase of tetragonal zirconia. Thus, in the remaining paper, heat-treated ZrO_2 is referred to as monoclinic zirconia, and the Y-TZP series is referred to as tetragonal zirconia. Heat treatment enabled the preparation of both monoclinic and tetragonal zirconia powders, and the composition of these samples was then examined.

Table 1 summarizes the chemical composition of the samples measured by XRF. No significant difference in the chemical composition was observed before and after heat treatment across all samples. The Y_2O_3 content obtained from XRF measurements was compared with the manufacturer-specified values, yielding an approximate curve. The plotted values, both before and after heat treatment, adhered to the approximate curve, and the Y_2O_3 contents of samples measured by the XRF instrument were consistent with those reported by the manufacturer.[16,27]

Moreover, the fine structures of zirconia samples were evaluated. Fig. 3 shows SEM micrographs of the zirconia samples post-immersion. All zirconia powders exhibited a secondary particle structure with primary particles being smaller than

Table 1 Elemental composition of the zirconia samples by XRF (mean ± SD, $n = 3$)

	Elemental composition (wt%)					
	Before heat treatment			After heat treatment		
Sample	ZrO_2	Y_2O_3	HfO_2	ZrO_2	Y_2O_3	HfO_2
ZrO_2	97.32 ± 0.02	0.17 ± 0.04	2.51 ± 0.06	97.30 ± 0.06	0.10 ± 0.07	2.61 ± 0.02
3Y-TZP	91.76 ± 0.03	5.78 ± 0.03	2.45 ± 0.05	91.86 ± 0.04	5.81 ± 0.01	2.34 ± 0.04
4Y-TZP	90.13 ± 0.05	7.49 ± 0.05	2.38 ± 0.02	90.24 ± 0.03	7.48 ± 0.00	2.29 ± 0.03
6Y-TZP	87.55 ± 0.03	10.11 ± 0.02	2.34 ± 0.02	87.46 ± 0.06	10.17 ± 0.03	2.38 ± 0.04

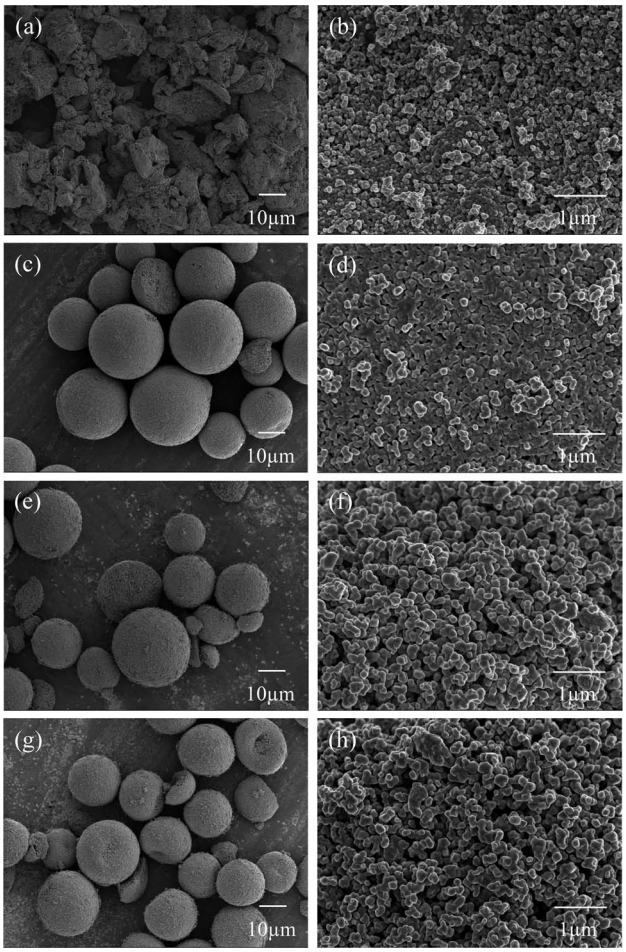

Fig. 3 SEM micrographs of the heat-treated zirconia samples. (a) and (b) ZrO_2 (monoclinic) after heat treated at 600 °C. (c) and (d) 3Y-TZP after heat treated at 1100 °C. (e) and (f) 4Y-TZP after heat treated at 1100 °C. (g) and (h) 6Y-TZP after heat treated at 1100 °C.

500 nm. In the monoclinic zirconia sample, the secondary particles were somewhat non-uniform in size and morphology. In contrast, the secondary particles of tetragonal zirconia were uniformly shaped and spherical.

The BET method was used to determine the specific surface area of the samples, considering their microstructure and particle size (Table 2). The specific surface areas of tetragonal zirconia were 2–3 times larger than those of monoclinic zirconia. Among the tetragonal zirconia samples, 3Y-TZP and 4Y-TZP had larger specific surface areas compared with 6Y-TZP.

Table 3 lists the pH values for each solution before and after zirconia immersion. All solutions in which the zirconia powder samples were immersed maintained a neutral pH range, simulating physiological conditions in the oral cavity.

CHN analysis was indicated to evaluate the number of antibacterial molecules adsorbed on the zirconia samples and the C content was measured. Fig. 4(a) shows the C content adsorbed per unit area of zirconia powder immersed in each solution. A comparison of the results for monoclinic and tetragonal zirconia in CPC- and BKC-containing PBS indicated that the monoclinic zirconia sample adsorbed 5–6 times more C content than the tetragonal zirconia samples. A two-way ANOVA ($\alpha = 0.05$) showed that the monoclinic zirconia sample was significantly different from all tetragonal zirconia samples. Notably, the monoclinic zirconia sample adsorbed approximately five times more antibacterial molecules per unit area than the tetragonal zirconia samples.

By the way, we performed FT-IR measurements to evaluate attached mode of CPC and BKC. However, we obtained only little signals of antibacterial agents. Therefore, we placed the measured results as ESI.†

Fig. 5 shows the DTA curves of the samples. For monoclinic ZrO_2, a clear peak indicating an exothermic change was observed at approximately 300 °C for both CPC and BKC, and similar peaks were observed in the tetragonal zirconia sample. Overall, the desorption temperatures of tetragonal zirconia samples were slightly lower than those of the monoclinic samples. Several exothermic peaks were observed in the 3Y-TZP sample with CPC. Therefore, the observed higher temperature desorption of monoclinic zirconia compared to tetragonal zirconia suggests that the antibacterial molecules are more tightly adsorbed.

Table 2 Specific surface area of the heat-treated zirconia samples (mean, $n = 2$)

Sample	Specific surface area ($m^2\ g^{-1}$)
ZrO_2	08.7
3Y-TZP	24.1
4Y-TZP	26.3
6Y-TZP	16.2

Table 3 pH values of the PBS solutions with and without antibacterial agents

Sample	PBS alone	PBS with CPC	PBS with BKC
Control	7.12	7.17	6.98
ZrO_2	7.34	7.40	7.14
3Y-TZP	7.27	7.35	7.14
4Y-TZP	7.28	7.32	7.13
6Y-TZP	7.28	7.33	7.09

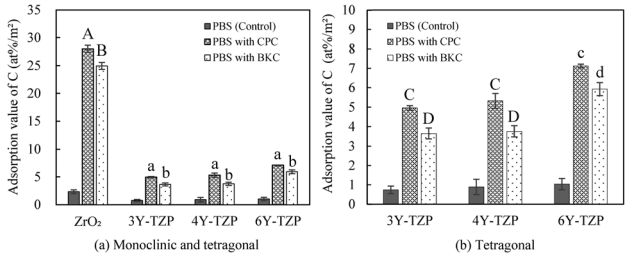

Fig. 4 Amount of carbon adsorption per unit area on the monoclinic and tetragonal samples (a) and the tetragonal samples (b) after immersion test. Upper case letters are significantly different from lower case letters ($p < 0.05$).

Commercial dental zirconia, which is expected to exhibit enough mechanical strength, is mostly tetragonal and is thus doped with stabilizing elements such as Y_2O_3.[16] Fig. 4(b) shows the amount of C adsorbed per unit area on the tetragonal zirconia powder. Interestingly, among the tetragonal zirconia samples, the amount of C adsorption tended to increase slightly as the Y_2O_3 content in the zirconia increased. Although 6Y-TZP was significantly different from 3Y-TZP and 4Y-TZP, no significant difference was observed between 3Y-TZP and 4Y-TZP. In general, REE can form complexes with quaternary amines[28] such as CPC and BKC. Thus, the increase in the Y_2O_3 content in zirconia likely led to an increase in the amount of Y_2O_3 complexes formed with CPC and BKC.

Next, we examined the influence of crystal structures of zirconia on the adsorption of antibacterial materials. To this end, we explored the effect of Y_2O_3 content in tetragonal zirconia. Based on the C adsorption contents of 3Y-TZP, 4Y-TZP, and 6Y-TZP tetragonal zirconia samples, theoretical values of C adsorption contents for tetragonal zirconia without Y_2O_3 could be determined through linear approximation. These theoretical values for CPC- and BKC-containing PBS were 2.1 wt% m^{-2} and 0.5 wt% m^{-2}, respectively. However, in our experiments, monoclinic zirconia adsorbed 28.9 wt% m^{-2} and 25.7 wt% m^{-2} of C when immersed in CPC- and BKC-containing PBS, respectively, approximately 11 and 26 times higher than the predicted values for tetragonal zirconia. This outcome suggests that monoclinic zirconia could adsorb significantly more antibacterial molecules than tetragonal zirconia in oral conditions, even after excluding the effect of stabilizing elements.

Surface properties, especially surface charge, significantly influence the adsorption of substances onto solid materials.[29,30] To examine the adsorption properties in solution, we focused on the potential of the sample surface. Previously, the zeta potential of the sample was measured.[31,32] Fig. 6 shows the zeta

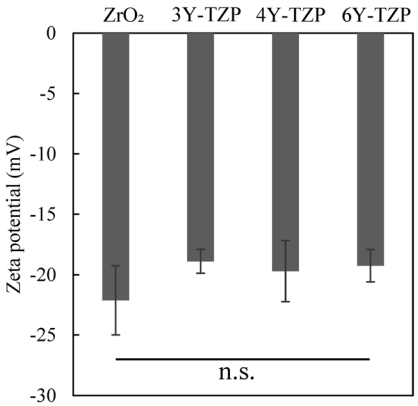

Fig. 6 Zeta potential of the zirconia samples in PBS after immersion test ($n = 3$). Error bars denote standard deviation.

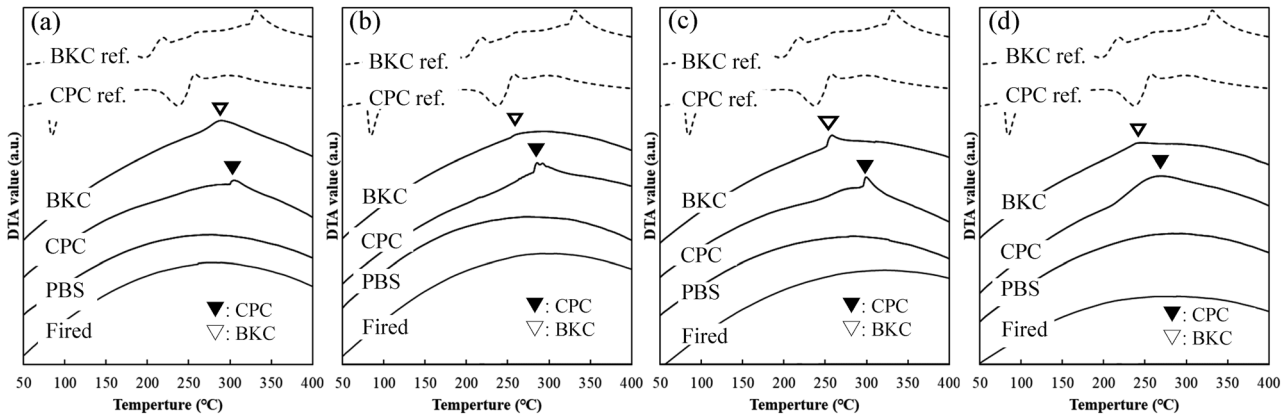

Fig. 5 DTA curves of each zirconia sample immersed in PBS, CPC, and BKC. (a) ZrO_2, (b) 3Y-TZP, (c) 4Y-TZP, and (d) 6Y-TZP. The CPC and BKC references are indicated by the dotted lines. The inverted triangular marks indicate the significant peaks of each sample immersed in CPC and BKC.

potential of each zirconia in PBS solution. The values for monoclinic zirconia, 3Y-TZP, 4Y-TZP, and 6Y-TZP in PBS were −22.11 mV, −18.89 mV, −19.70 mV, and −19.25 mV, respectively. The surfaces of all samples were negatively charged, and the values for monoclinic and tetragonal zirconia were comparable, and consistent with those reported previously.[33,34]

Although no significant difference was observed in the bulk zeta potential between monoclinic and tetragonal phases, the exposed crystal planes in both zirconia crystals are inherently different. The results can likely be explained by the fact that the more negatively charged crystal faces exposed on the less symmetrical monoclinic zirconia crystals contribute significantly to the adsorption of antibacterial molecules.

As shown in Fig. 7(a), the samples immersed in BKC showed a zone of inhibition. In contrast, the samples without immersion in BKC (70% ethanol immersion) showed no formation of an inhibition zone. Fig. 7(b) shows that 6Y-TZP exhibited a slightly larger inhibition zone than 4Y-TZP. However, the difference was not significant. These results suggest that zirconia with adsorbed antibacterial molecules exhibits antibacterial properties.

We observed that monoclinic zirconia adsorbed significantly more antibacterial molecules than tetragonal zirconia. Although dental zirconia is primarily tetragonal, damaged areas such as microcracks induced by aging can undergo phase transformation and become monoclinic.[35] Traditionally, restorations that have been in the oral cavity for an extended period require regular maintenance and remanufacturing, given the significant risk of secondary caries resulting from marginal leakage caused by occlusal pressure, wear, and material degradation.[36,37] However, the results of this study suggest that the monoclinic zirconia crystals in long-term zirconia restorations adsorbed a greater number of antibacterial molecules, resulting in improved antibacterial activity. Additionally, in highly translucent zirconia, characterized by high Y_2O_3 contents, the adsorption effect of stabilizing elements is further augmented. This discovery holds significant implications for the dental materials and can promote the development of treatment methods for patients experiencing oral-care challenges, especially elderly patients. Because it is difficult for elderly people to perform proper dental care, the interaction between Y_2O_3 and its antibacterial effects, which was clarified in this study, could be applied to prevent dental caries, periodontal disease, and aspiration pneumonia in the elderly.

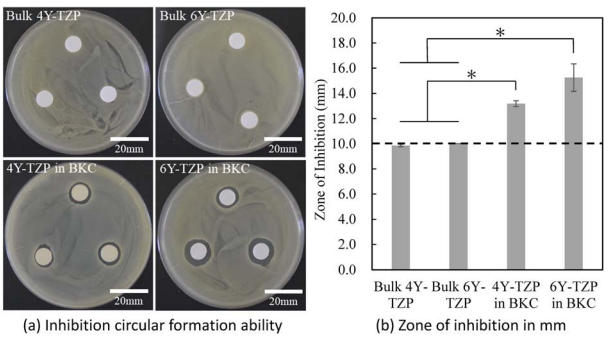

(a) Inhibition circular formation ability (b) Zone of inhibition in mm

Fig. 7 Results of the antibacterial activity test of 4Y-TZP and 6Y-TZP absorbed with and without BKC against *S. aureus* ($n = 3$). (a) Inhibition circular formation ability, (b) zone of inhibition in mm. The dotted line on (b) denotes the disc diameter. *: $p < 0.05$.

Conclusion

This study was aimed at evaluating the ability of tetragonal and monoclinic zirconia crystal systems to support antibacterial molecules in simulated oral environments. Monoclinic zirconia was noted to adsorb approximately five times more antibacterial molecules (CPC and BKC) compared with tetragonal zirconia.

In tetragonal zirconia, the amounts of CPC and BKC adsorbed slightly increased as the Y_2O_3 content in zirconia increased. This phenomenon likely occurred because Y_2O_3 in zirconia forms complexes with quaternary amines such as CPC and BKC.

Data availability

The authors confirm that the data supporting the findings of this study are available within the article and its ESI.†

Author contributions

Mihiro Itotagawa: investigation, data curation, writing-review & editing-original draft, funding acquisition Hiroshi Kono: investigation, data curation, writing-review & editing Tadahiro Higashinakao: investigation, writing-review & editing Yuki Sugiura: investigation, methodology, data curation, writing-review & editing, conceptualization Yuta Otsuka: methodology, writing-review & editing Masafumi Kikuchi: supervision, writing-review & editing Yoshihiro Nishitani: supervision, writing-review & editing.

Conflicts of interest

The authors declare that they have no known competing financial interests or personal relationships that could have appeared to influence the work reported in this paper.

Acknowledgements

This work was partially supported by JSPS KAKENHI (Grant number JP22K10040 and JP23K09235) and AMED (Grant number JP23ym0126811j0002). The authors thank Mr. Shingo Kubo, Division of Instrumental Analysis, Centre for Advanced Science Research and Promotion, Kagoshima University, and Prof. Yasuro Niidome, Faculty of Science, Kagoshima University, for providing valuable comments and technical support.

Notes and references

1 Y. Zhang and B. R. Lawn, *J. Dent. Res.*, 2018, **97**, 140–147.
2 M. M. Lobo, R. B. Gonçalves, G. M. B. Ambrosano and L. A. F. Pimenta, *J. Biomed. Mater. Res. B Appl. Biomater.*, 2005, **74**, 725–731.

3 L. Cheng, M. D. Weir, K. Zhang, D. D. Arola, X. Zhou and H. H. K. Xu, *J. Dent.*, 2013, **41**, 345–355.
4 A. R. Peris, F. H. O. Mitsui, M. M. Lobo, A. K. B. Bedran-russo and G. M. Marchi, *Dent. Mater.*, 2007, **23**, 308–316.
5 N. Zhang, M. A. S. Melo, C. Chen, J. Liu, M. D. Weir, Y. Bai and H. H. K. Xu, *Dent. Mater.*, 2015, **31**, 1119–1131.
6 F. J. Burke and P. S. Lucarotti, *J. Dent.*, 2009, **37**, 12–24.
7 B. Van Meerbeek, M. Peumans, A. Poitevin, A. Mine, A. Van Ende, A. Neves and J. De Munck, *Dent. Mater.*, 2010, **26**, e100–e121.
8 I. Denry and J. R. Kelly, *Dent. Mater.*, 2008, **24**, 299–307.
9 I. Dion, L. Bordenave, F. Lefebvre, R. Bareille, C. Baquey, J.-R. Monties and P. Havlik, *J. Mater. Sci.: Mater. Med.*, 1994, **5**, 18–24.
10 C. Piconi and G. Maccauro, *Biomaterials*, 1999, **20**, 1–25.
11 R. H. J. Hannink, P. M. Kelly and B. C. Muddle, *J. Am. Ceram. Soc.*, 2000, **83**, 461–487.
12 A. J. Raigrodski, *J. Prosthet. Dent.*, 2004, **92**, 557–562.
13 M. Yoshimura, *Am. Ceram. Soc. Bull.*, 1988, **67**, 12–17.
14 K. Momma and F. Izumi, *J. Appl. Crystallogr.*, 2011, **44**, 1272–1276.
15 P. Li, I. W. Chen and J. E. Penner-Hahn, *J. Am. Ceram. Soc.*, 1994, **77**, 1281–1288.
16 S. Amano, H. Fujisaki, H. Nagayama and S. Azechi, *Tosoh Res. Technol. Rev.*, 2019, **63**, 61–65.
17 J. Chevalier, L. Gremillard, A. V. Virkar and D. R. Clarke, *J. Am. Ceram. Soc.*, 2009, **92**, 1901–1920.
18 A. Loganathan and A. S. Gandhi, *Mater. Sci. Eng., A*, 2012, **556**, 927–935.
19 R. C. Garvie, R. H. Hannink and R. T. Pascoe, *Nature*, 1975, **258**, 703–704.
20 J. M. Antonucci, D. N. Zeiger, K. Tang, S. Lin-Gibson, B. O. Fowler and N. J. Lin, *Dent. Mater.*, 2012, **28**, 219–228.
21 S. Takenaka, T. Ohsumi and Y. Noiri, *Jpn. Dent. Sci. Rev.*, 2019, **55**, 33–40.
22 F. A. Pitten and A. Kramer, *Arzneim.-Forsch.*, 2001, **51**, 588–595.
23 B. Lygo and B. I. Andrews, *Acc. Chem. Res.*, 2004, **37**, 518–525.
24 W. J. Maeck, G. L. Booman, M. E. Kussy and J. E. Rein, *Anal. Chem.*, 1961, **33**, 1775–1780.
25 C. Zhang, Y. Liu, S. Kang, F. Yan, Z. Hu, P. Chen, G. Huang, C. Li and A. Stubbins, *Environ. Sci. Technol.*, 2024, **58**(22), 9731–9740.
26 S. Brunauer, P. H. Emmett and E. Teller, *J. Am. Chem. Soc.*, 1938, **60**, 309–319.
27 H. Fujisaki, K. Kawamura and K. Imai, *Tosoh Res. Technol. Rev.*, 2012, **56**, 57–61.
28 S. Guo, M. Ma, Y. Wang, J. Wang, Y. Jiang, R. Duan, Z. Lei, S. Wang, Y. He and Z. Liu, *Chem. Rev.*, 2024, **124**(11), 6952–7006.
29 G. Decher, J. D. Hong and J. Schmitt, *Thin Solid Films*, 1992, **210**, 831–835.
30 M. Rabe, D. Verdes and S. Seeger, *Adv. Colloid Interface Sci.*, 2011, **162**, 87–106.
31 R. Greenwood and K. Kendall, *J. Eur. Ceram. Soc.*, 1999, **19**, 479–488.
32 D. Hanaor, M. Michelazzi, C. Leonelli and C. C. Sorrell, *J. Eur. Ceram. Soc.*, 2012, **32**, 235–244.
33 W. Hertl, *Langmuir*, 1989, **5**, 96–100.
34 T. Fengqiu, H. Xiaoxian, Z. Yufeng and G. Jingkun, *Ceram. Int.*, 2000, **26**, 93–97.
35 M. Guazzato, M. Albakry, S. P. Ringer and M. V. Swain, *Dent. Mater.*, 2004, **20**, 449–456.
36 I. R. Blum, C. D. Lynch and N. H. Wilson, *Clin., Cosmet. Invest. Dent.*, 2014, **6**, 81–87.
37 H. Askar, J. Krois, G. Göstemeyer, P. Bottenberg, D. Zero, A. Banerjee and F. Schwendicke, *Clin. Oral Invest.*, 2020, **24**, 1869–1876.